How Nascent Structure of Semicrystalline Polymer Powders Enhances Bulk Mechanical Properties

D. Jauffrès,[†] O. Lame,*[,†] G. Vigier,[†] and F. Doré[‡]

MATEIS, INSA-Lyon, CNRS UMR5510, Bât. B. Pascal 7 Avenue Jean Capelle, F-69621 Villeurbanne cedex, France, and CETIM, 7 rue de la presse, BP802, F-42952 Saint Etienne cedex 9, France

Received May 21, 2008; Revised Manuscript Received October 31, 2008

ABSTRACT: For the first time, bulk material containing high fraction of nascent phase has been processed and analyzed. The obtained materials are "auto-composites" composed of nascent and recrystallized polymer. Obtaining such materials has been made possible thanks to high velocity compaction (HVC). Contrary to conventional processes, HVC allows obtaining a chosen fraction of nascent polymer in bulk materials. Polyoxymethylene (POM) and ultra high molecular weight polyethylene (UHMWPE) nascent powders have been processed by HVC. In this study, the semicrystalline nanostructure and the molecular topology (tie molecules and entangled loops) of the materials are discussed. A specific attention is paid to the nascent nanostructure of POM and UHMWPE. The modifications occurring within nascent phase during HVC have been addressed and the differences between nascent POM and nascent UHMPWE are emphasized. Finally, the mechanical properties of HVC materials are discussed in relation with material micro and nanostructures.

1. Introduction

Nascent or as-polymerized refers to the state of the polymer directly after its polymerization, before any subsequent operation involving melting, such as pelletization. Nascent semicrystalline polymers come in powder form and are generally characterized by a particularly high crystallinity, hardly accessible by crystallization from the melt.[1−4] Nascent structures of semicrystalline polymers and their formation have not interested many researchers, mainly because quasi-all processing methods involve a melting stage and "bulk" nascent polymer with valuable strength is impossible to obtain. However, the few papers available concerning nascent semicrystalline polymers show that their structure would be very different from that of melt-crystallized materials.[3,5−8]

High velocity compaction (HVC) is an innovative process developed that allows the processing of nascent semicrystalline powders via sintering. It consists in applying several controlled energy impacts to a heated (∼20 °C below the polymer melting temperature) and powder-filled die. The repeated impacts provoke self-heating, preferentially at particle interfaces, which induces local melting. The welding of the particles is then provided by the subsequent recrystallization of the melted fraction of the polymer.[9,10] Important drawbacks of conventional melt-processing, caused by the complete melting stage, such as shrinkage, cavity formation or chemical degradation, are thus limited by the use of HVC. In addition, HVC allows the processing of nonmelt processable polymers within a short processing time compared to conventional sintering of these polymers. A semicrystalline polymer with high shrinkage and high sensitivity to degradation, polyoxymethylene (POM), and a nonmelt processable semicrystalline polymer, ultra high molecular weight polyethylene (UHMWPE), have been processed by HVC. Mechanical and physical characterization of the materials obtained have been reported previously.[10,11]

After local melting provoked by the impacts, the melted fraction of polymer recrystallizes with a cristallinity degree lower than at its nascent state. It follows that HVC material is composed at the micrometer scale of two distinct fractions of the same polymer that differ in their crystallinities and semicrystalline nanostructures, even if they keep the same crystallographic cell. These two fractions will be referred as phases, i.e. the "nascent" phase and the "recrystallized" phase. The nature of the phase (nascent or recrystallized) depends on the temperature reached locally within the material. The fraction of recrystallized phase f_R contained in a HVC processed polymer is controlled by the processing parameters (temperature, impact energy and number of impacts) and can be estimated from the overall crystallinity degree obtained by DSC.[11] It has been established that the recrystallized phase is preferentially located at particle interfaces, owing to a more significant self-heating in these zones.[9] Consequently HVC polymer can be seen as an "auto-composite" comprise of a nascent phase embedded in recrystallized phase acting as a matrix. HVC materials have thus a two-scale structure since the two semicrystalline phases are also composed at the nanometer scale of crystallites separated by amorphous regions.

A significant amount of nascent material is retained during the HVC process, allowing us for the first time to investigate the mechanical properties resulting from the specific structure of nascent polymers. Both HVC UHMWPE and HVC POM exhibit an increased stiffness. Regarding mechanical behavior, HVC POM reveals to be always brittle at 20 °C, even in compressive stress state, while HVC UHMWPE is ductile and exhibits significant true fracture strains. This difference is suspected to originate in nascent properties of materials. In particular, nascent POM seems to be intrinsically brittle.[10]

The characteristics of nascent semicrystalline nanostructure, i.e. the crystallinity degree, the size, morphology and arrangement of the crystallites and the molecular topology govern the mechanical properties of semicrystalline polymers.[12−14] Previous studies have reported that nascent UHMWPE has rather small crystallites compared to thick crystallites generally observed in melt-crystallized UHMWPE.[15−17] Nascent UHMWPE amorphous phase presents topological constrains which likely results from of the simultaneous polymerization and crystallization; they are lost after the first melting.[18,19] In the case of nascent POM, Small angle X-ray scattering performed by Al Jebawi et al. have shown that the structure would be very disordered and that

* Corresponding author. E-mail: Olivier.lame@insa-lyon.fr.
[†] MATEIS, INSA-Lyon, CNRS UMR5510.
[‡] CETIM.

10.1021/ma801133v CCC: $40.75
Published on Web 11/18/2008

crystallite thicknesses would be similar to that of melt-crystallized material.[20,21] Unfortunately, nascent polymer molecular topology, in particular the density of intercrystalline links (i.e., tie molecules and entangled loops), has never been comprehensively addressed.

Lack of data concerning nascent structures of POM and UHMWPE, as well as questioning about their evolution during HVC, have motivated a more in-depth study.

Size, morphology and arrangement of the crystallites have been characterized by SAXS and atomic force microscopy (AFM) for the nascent powders and the HVC materials. In the following "microstructure" refers to the crystallite organization up to the micrometric scale of the nascent phase or the recrystallized phases whereas "nanostructure" refers to the arrangement at the nanometric scale of the crystallites within a given phase. It is attempted to indirectly evaluate the density of intercrystalline links of HVC materials. These new results, added to our knowledge of the structure at the micrometer scale[10,11] allow us to completely describe HVC material structure. Finally, the relationships between mechanical properties and micro/nanostructure of HVC materials can be addressed with emphasize on differences between POM and UHMWPE.

2. Materials and Methods

2.1. Materials. The UHMWPE nascent powder used as starting material for HVC processing is a commercial powder, GUR 4113, produced by Ticona (Oberhausen, Germany). The viscosity average molecular weight of this PE is reported to be 3.9 million g/mol by Ticona.

As for POM, a nascent powder of Delrin grade 500 (molecular weight = 45 000 g/mol) was graciously provided to us by Dupont (Le Grand Saconnex, Switzerland).

As references, POM and UHMWPE processed by compression molding have been studied. Delrin500 has been molded in our laboratory while a commercial melt-crystallized UHMWPE processed by PolyHySolidur (Vreden, Germany) has been used.

The HVC processed materials are designated by their recrystallized phase fraction f_R obtained from previously published DSC results.[10,11]

2.2. SAXS. SAXS experiments were performed on a laboratory bench equipped with a 2D CCD camera. The Cu Kα radiation (wavelength $\lambda = 0.154$ nm) was selected from a Rigaku (Tokyo, Japan) rotating anode and collimated owing to a specific point-focusing Goebel mirror from Xenocs (Grenoble, France). HVC materials exhibit SAXS patterns with uniform rings which is characteristic of isotropic materials. Indeed, die compaction does not induce strong anisotropic deformation so that isotropic nanostructure appears. An azimuthal integration of the patterns can thus be performed to obtain the scattering intensities as a function of the scattering angles 2θ.

After spectrum treatments,[22] the average long period L_p of the scattering lamella stacks was calculated by Bragg's law:

$$L_p = \frac{2\pi}{q_{peak}} \tag{1}$$

where q_{peak} is the norm of the scattering vector at the peak intensity. The DSC crystal volume fraction Φ_c was used to obtain an estimation of crystal and amorphous thicknesses l_c and l_a:

$$\Phi_c = X_c \frac{\rho_a}{\rho_c - X_c(\rho_c - \rho_a)} \quad \text{with} \quad X_c = \frac{\Delta H_m}{\Delta H_m^0} \tag{2}$$

$$l_c = \Phi_c L_p \quad \text{and} \quad l_a = L_p - l_c \tag{3}$$

ΔH_m is the sample melting enthalpy (corresponding to the melting peak area) and ΔH_m^0 the melting enthalpy of a perfect crystal, i.e., 247 J/g for POM and 290 J/g for PE.[23,24] DSC results are presented elsewhere[10,11]

For crystal and amorphous densities, we used the following values: $\rho_c = 1.49$ and $\rho_a = 1.21$ for POM, and $\rho_c = 0.999$ and $\rho_a = 0.855$ for UHMWPE.[23,24]

The correlation function approach[25,26] was used to evaluate the local crystallinity in the lamellae stacks $\Phi_{c_{st}}$ and also l_c and l_a independently from DSC data.

$$l_c = \Phi_{c_{st}} L_p \quad \text{and} \quad l_a = L_p - l_c \tag{4}$$

2.3. Atomic Force Microscopy. A Veeco (Santa Barbara, CA) NanoScope Dimension 3100 was used in tapping mode with tips oscillating in air at a frequency close to the cantilever resonance frequency (~300 kHz). The viscoelastic properties of the material are probed, and thus the phase image allows the differentiation of crystalline and amorphous regions.[27] Under the conditions used (i.e., moderate tapping), the harder component (crystal) appears bright while the softer one (amorphous material) appears dark. Extremely flat surfaces were prepared by ultramicrotomy at −110 °C. Nascent powders were embedded in epoxy resin before being microtomed. To choose the images which have been analyzed and presented in this paper, several zone at several scale have been observed. The analysis relies on the images giving a lamellae size compatible with the SAXS measurements. In this case, it is assumed that the cut plane is nearly perpendicular to the crystallites. It corresponds to lower size that can be observed on AFM images. In addition, a second criterion is used: the chosen image has to be qualitatively representative of most of the AFM images obtained on a same sample. The main purpose of the AFM is to allow the characterization of the nascent and the recrystallized phases within a HVC sample as SAXS cannot independently characterize these two phases and provide only a sum of the contribution of each phase.

SAXS and AFM are complementary techniques: SAXS leads to average characteristics sizes at a nanometric scale over a large volume (1 mm^3) whereas AFM gives a qualitative idea of the crystallite organization from few nanometers to few micrometers in a localized zone.

2.4. Compression Tests. Uniaxial compression tests were carried out to investigate intrinsic material behavior. The compressive stress state limits premature failure of the sample due to sintering defects, and thus effectively allows the characterization of HVC material intrinsic behavior.

Ten mm height parallelepiped samples (section 6 mm × 6 mm) were compressed between two steel plates at a strain rate of 2×10^{-3} s^{-1}. The surfaces between the sample and the plates were lubricated to have the more homogeneous deformation possible. True stress and true strain were evaluated from the measured displacement and force. Five compression tests were conducted to check the repeatability and only one representative test is presented here.

2.5. Low Voltage Scanning Electron Microscopy. An FEI XL-30 ESEM FEG (Hillsboro, OR) was used at low accelerating voltage to observe nascent particles. The use of low voltage (between 0.8 kV and 1.4 kV) allows the observation of nonconductive samples without metal coating.

3. Structures of HVC and Nascent Materials

3.1. UHMWPE. *SAXS.* SAXS experiments were carried out to investigate UHMWPE nascent nanostructures before and after HVC. Nascent powders give rise to a significant increase in SAXS intensity at low angles, owing to scattering by micrometric cavities and/or globular structure,[28] that completely masks any scattering by crystallites. Consequently, SAXS has been performed on a compacted UHMWPE nascent powder to reduce

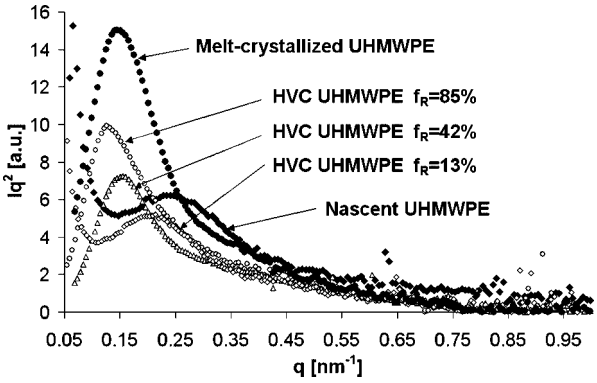

Figure 1. Lorentz-corrected SAXS intensity profiles for nascent, melt-crystallized, and selected HVC UHMWPE.

Table 1. UHMWPE Structural Parameters from Bragg's Law

	L_p (nm) [Bragg] ± 3%	Φ_c [DSC] ± 2%	l_c (nm) [Bragg] ± 5%	l_a (nm) [Bragg] ± 5%
nascent UHMWPE	26	0.61	16	10
melt-crystallized UHMWPE	42	0.47	20	22

Table 2. UHMWPE Structural Parameters from Correlation Function

	L_p (nm) [CF] ± 3%	$\Phi_{c_{st}}$ [CF] ± 4%	l_c (nm) [CF] ± 4%	l_a (nm) [CF] ± 4%
nascent UHMWPE	24	0.82	20	4
melt-crystallized UHMWPE	38	0.74	28	10

the scattering due to porosity and/or globular structure and to reveal the scattering by crystallites. SAXS profiles recorded for nascent UHMWPE, melt-crystallized UHMWPE and three selected HVC UHMWPE are presented in Figure 1. For nascent and melt-crystallized samples, nanostructural parameters (long period L_p, crystal thickness l_c, and amorphous thickness l_a) have been extracted using Bragg's law (Table 1) and correlation function approach (Table 2).

SAXS peaks are not very pronounced and it was even not possible to distinguish a correlation peak before applying the Lorentz correction, which denotes a very low degree of order for the five samples.[29,30] For melt-crystallized sample, it is believed that crystallization in regularly stacked lamellae is hindered by the extremely high molecular weight.[29] The disorder of the structure seems to be higher for nascent and low f_R HVC samples as they exhibit lower scattering intensity from lamella stacks. One could also argue that weaker peaks of these samples originate in their higher crystallinity degree, since scattering peak intensity varies with $\Phi_{c_{st}}(1 - \Phi_{c_{st}})$,[25,31] but this effect would only account for a 10−20% intensity decrease.

It is observed that the nascent crystallites are thinner than the melt-crystallized ones, which corroborates the recent explanation proposed for nascent UHMWPE high melting point.[18,19] In Table 2, it is noted that the local crystal volume fraction in the stacks ($\Phi_{c_{st}}$) is higher than the global crystal volume fraction (Φ_c). It is a classical result, and an interpretation generally proposed is that pockets of amorphous phase are excluded from the stacks.[25,32] Consequently, the most relevant value for crystal thickness should be the one calculated by the correlation function approach, i.e., around 20 nm for nascent UHMWPE and around 30 nm for melt-crystallized UHMWPE.

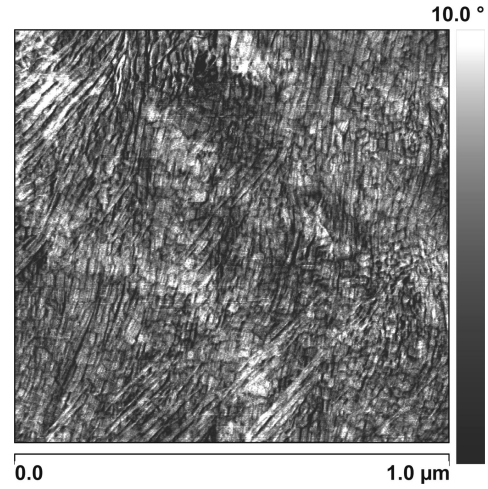

Figure 2. AFM phase image of nascent UHMWPE powder.

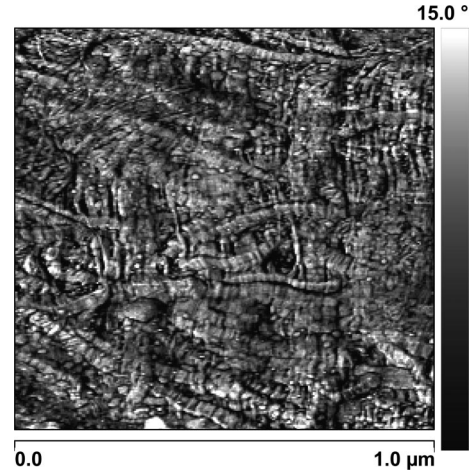

Figure 3. AFM phase image of melt-crystallized UHMWPE (obtained by compression molding).

Analysis of HVC materials SAXS profiles (displayed in Figure 1) is not obvious as both nascent and melt-crystallized phases contribute to the scattering and there are probably two lamella populations. Consequently, in our point of view, it is not relevant to extract structural parameters from these profiles. However, some qualitative comments can be done. SAXS profiles of HVC UHMWPE show a progressive shift of the correlation peak toward low q that can be attributed to:

- The appearance of the melt-crystallized phase contribution that exhibits a higher L_p.
- A possible increase in the crystallite average thickness within the nascent phase, since $l_c = \Phi_c L_p$.

A crystal thickening of the nascent phase during HVC would not be surprising regarding the high temperature and pressure involved, but this needs to be confirmed by AFM observation as the SAXS peak shift could be explained only by the recrystallized phase contribution.

It is also noted that high scattering intensity at low q completely disappears if the amount of recrystallized phase is sufficiently high, which reveals that the pores and/or globular structure causing this scattering progressively disappear during HVC.

AFM. AFM was first carried out on surfaces of nascent and melt-crystallized UHMWPE (Figure 2 and 3). As explained previously, the image in Figure 2 has been chosen so that it is representative of the microstructure and the average crystallite thickness is close to the measurements obtained by SAXS. A

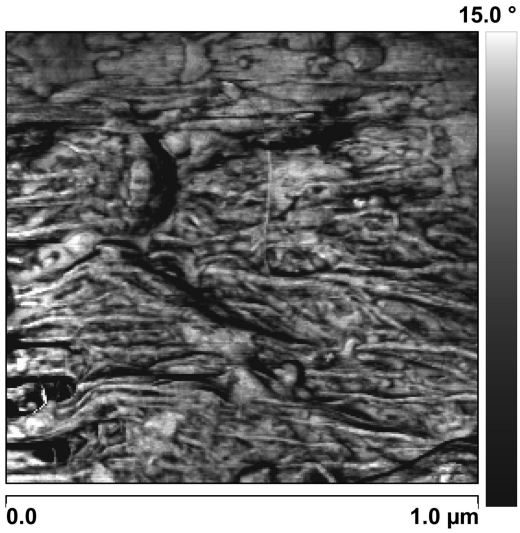

Figure 4. AFM phase image of HVC UHMWPE at $f_R = 85\%$. Nascent phase zone.

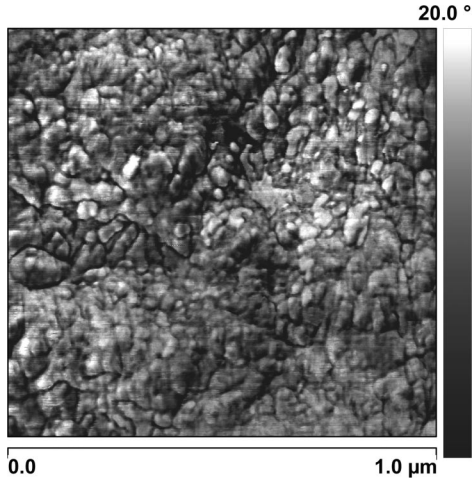

Figure 5. AFM phase image of HVC UHMWPE at $f_R = 85\%$. Recrystallized phase zone.

lamellar structure can be easily observed even if SAXS measurements suggest that nascent UHMWPE lamellae are not regularly distributed (SAXS peak weakly pronounced). Indeed, even if the microstructure appears rather regular at a micrometeric scale, lamella size distribution is wide. This observation is thus compatible with SAXS experiments.

In Figure 3, the same kinds of observations have been carried out on melt-recrystallized UHMWPE. Again, a representative image has been chosen using the same procedure. On this image the microstructure remains lamellar with a wide range of object size. It appears more disordered than the nascent UHMWPE powder; however some lamellae seem to be gathered to form higher size objects. These observations are in agreement with SAXS experiments (SAXS correlation peak more pronounced), it would indicate that lamella stack is locally better than it appears at higher scale observation.

Then the two different phases have been observed on a same HVC sample. Figure 4 shows the nascent phase while Figure 5 shows the recrystallized phase in the same sample. It has been possible to distinguish recrystallized zones from nascent zones thanks to an optical contrast due to higher roughness of nascent phase that likely originates in internal stresses relaxation after microtomy.[33] It is noted that after HVC, the nascent phase shows thicker crystallites (Figure 4), likely resulting in a process similar

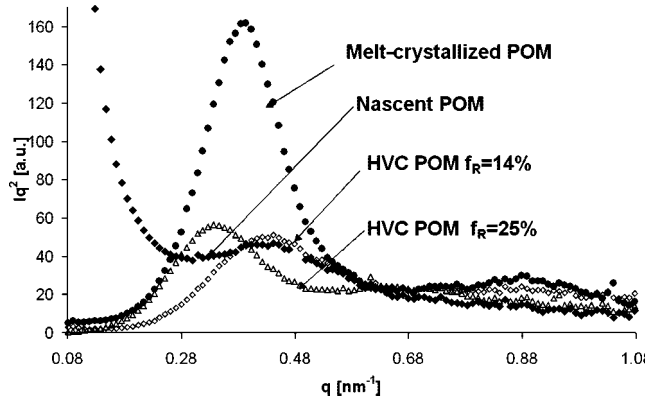

Figure 6. Lorentz-corrected SAXS profiles of nascent, melt-crystallized, and HVC POM.

to the thickening by annealing.[34] The existence of a thickening process during HVC, previously suspected from the SAXS results, is thus confirmed.

The recrystallized phase (Figure 5), formed after the local melting of the nascent polymer, keeps a disordered structure, likely because UHMWPE very high molecular weight hinders the reorganization during the recrystallization. It is noted that recrystallized UHMWPE within HVC material exhibits a particular granular structure that differs from the melt-crystallized morphology obtained by compression molding. For Strobl et al.[35,36] and Magonov[27] a granular structure can appear during the first stage of the crystallization, before the complete "joining" of the crystal blocks to form the lamellae. This particular structure could also be a result of crystal lamella fragmentation induced by the high compression stress undergone by the material during HVC.[37]

The differences between compression molded material and recrystallized phase structures could thus originate in different thermal histories or be a consequence of high stresses induced by the HVC.

In short, nascent UHMWPE exhibits a highly crystalline nanostructure characterized by a poorly ordered arrangement of rather small crystallites, significant topological constrains in amorphous phase and high porosity. Under HVC, porosity is eliminated and the average crystal thickness increases. Locally, a complete melting that leads to the lost of nascent phase specificities (i.e., high crystallinity and topological constrains) can occur. It follows that there is a progressive appearance of melted polymer within the sample during HVC, which will form the recrystallized phase after cooling and crystallization. Even if the crystallinity degree is not very different from a classical melt-recrystallized UHMWPE, the melt-recrystallized microstructure is strongly disordered and classical lamella structure is difficult to distinguish. This phenomenon is probably due to the fact that recrystallization is rather quick in HVC conditions compared to compression molding.

3.2. POM. The same approach has been used for the investigation of POM nascent structure and its modifications during HVC processing.

SAXS. Lorentz-corrected SAXS profiles obtained on nascent, melt-crystallized and HVC POM are displayed in Figure 6. SAXS profile of nascent POM powder is characterized by a significant intensity at low q, likely due to pores, which disappears after HVC.

The parameters calculated using Bragg's equation and DSC data are reported in Table 3, and the ones obtained by the correlation function approach are presented in Table 4. Similarly to UHMWPE, the parameters have only been extracted for nascent and melt-crystallized samples, as HVC POM profiles

Table 3. POM Structural Parameters from Bragg's Law

	L_p (nm) [Bragg] ± 3%	Φ_c [DSC] ± 2%	l_c (nm) [Bragg] ± 5%	l_a (nm) [Bragg] ± 5%
nascent POM	14.6	0.88	12.9	1.7
melt-crystallized POM	16.1	0.69	11.1	5.0

Table 4. POM Structural Parameters from Correlation Function

	L_p (nm) [CF] ± 3%	$\Phi_{c_{st}}$ [CF] ± 4%	l_c (nm) [CF] ± 4%	l_a (nm) [CF] ± 4%
nascent POM	14.6	0.77	11.2	3.4
melt-crystallized POM	15.6	0.76	11.8	3.8

correspond to the superimposed scattering of two different structures.

As seen in Table 3 and Table 4, POM Nascent and melt-crystallized crystal thicknesses are quite similar, which is in agreement with DSC results.[10]

In addition, it is worth noting that the local crystal volume fraction in the stacks (Φc_{st}) is lower than the global crystal volume fraction (Φc) for nascent POM. This is remarkable since the opposite ($\Phi c_{st} > \Phi c$) is generally observed, in particular for melt-crystallized POM, due to pockets of amorphous phase excluded from the stacks.[25,32] One explanation for $\Phi_{c_{st}} < \Phi_c$ could be that some highly crystalline regions of the material do not contribute to SAXS peak, probably owing to a noncorrelated structure.

As seen in Figure 6, nascent POM and HVC POM scattering intensities are very low compared to melt-crystallized ones. This could originate in a lower degree of order within the lamella stacks or in the crystallinity decrease (the integrated scattering intensity vary with $\Phi_{c_{st}}(1 - \Phi_{c_{st}})$).[25,30,31] Nascent and melt crystallized $\Phi_{c_{st}}$ values are closed and the higher crystallinity of nascent POM would only lead to an intensity decrease of 10%. Consequently, the lower lamella scattering intensity of nascent POM is mainly due to a more disordered crystal lamella arrangement.

It is now proposed to analyze the evolution of the SAXS profiles after HVC at different processing conditions. As for HVC UHMWPE, HVC POM shows a shift of the correlation peak toward lower q that could also originate in a combine effect of the following:

- Increased melt-crystallized phase contribution exhibits a slightly higher L_p.
- Crystal average thickness increases within the nascent phase.

This second phenomenon is significant and likely predominates as DSC results show a shift toward the high temperature of the melting peak.[10] As for UHMWPE, it is observed that for moderate f_R (up to 15−20%), HVC POM nascent phase nanostructure would be very similar to nascent powder one, as proved by comparable SAXS correlation peaks and DSC melting peaks.

AFM. Similarly to UHMWPE, nascent and melt-crystallized materials have first been observed and then it has been attempted to detect the modifications of the nascent structure within HVC POM. AFM images of nascent and melt-crystallized POM reveal two completely different structures (Figures 7 and 8). While melt-crystallized POM exhibits a conventional lamellar structure,[38] nascent POM shows a very particular structure formed of lamellae and crystal "blocks" that do not extend themselves in one particular plan. Nearly no information is available in the literature concerning this nanostructure as nascent POM has never been used until now. Depending on the polymerization conditions, the presence of "thick crystallites" has however been reported previously.[39] The observed blocks could correspond

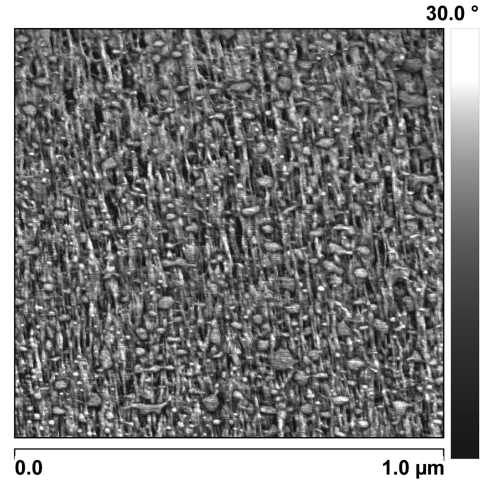

Figure 7. AFM phase image of nascent POM powder.

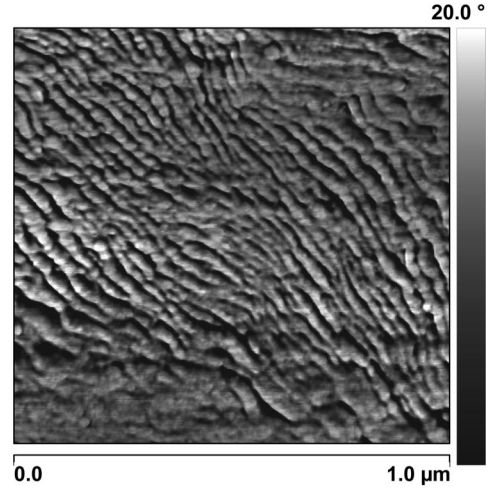

Figure 8. AFM phase image of melt-crystallized POM (obtained by compression molding).

to these "thick crystallites". This structure, highly disordered and with possibly uncorrelated crystal blocks is consistent with the weak SAXS peak and $\Phi_c > \Phi_{c_{st}}$.

Selected images from HVC POM nascent phase and HVC POM recrystallized phase are presented in Figures 9 and 10. HVC POM recrystallized zone exhibits a classical semicrystalline lamellar structure: a regular arrangement of lamellae which is similar to that of melt-crystallized POM. On the contrary, HVC POM nascent zone is disordered and the microstructure is very different from melt-recrystallized POM (for compression molding as well as for HVC). It presents a globular morphology closer to nascent structure. It is then probable that the nascent structure is partially retained after processing. However at few tens of nanometers scale, it seems rather coarser and thin lamellae of nascent structure have disappeared.

These AFM observations allow us to qualitatively confirm SAXS results concerning the degree of order and the evolution of lamella thicknesses.

Finally, nascent POM nanostructure appears to be similar to the nascent UHMWPE one: both materials exhibit a highly crystalline disordered nanostructure with rather small crystallites. However, nascent POM likely does not present the particularity of having topological constrains in its amorphous phase as it presents a conventional molecular weight.

For POM, recrystallized structure within HVC samples is similar to that of compression molded POM. On the contrary,

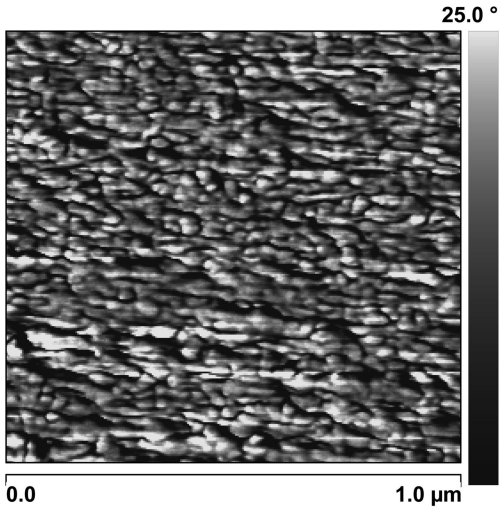

Figure 9. AFM phase image of POM HVC at $f_R = 14\%$. Nascent phase zone.

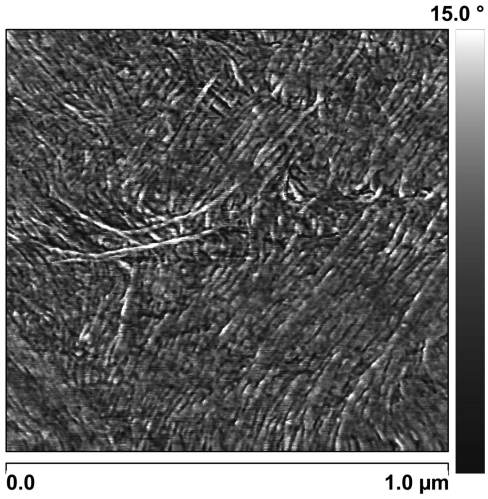

Figure 10. AFM phase image of POM HVC at $f_R = 14\%$. Recrystallized phase zone.

after HVC, UHMWPE recrystallized phase is significantly different from the compression molded nanostructure. This difference originates likely from the extremely high molecular weight of UHMWPE which prevents sufficient reorganization during the processing time. In addition, during HVC, an increase in the average crystal thickness occurs within the nascent phase, for both materials.

4. Molecular Topology

4.1. Intercrystalline Links. Regarding structure−mechanical property relationships, a very important aspect is the density of intercrystalline links, i.e. tie molecules and entangled loops. Intercrystalline links, by transmitting the stress between adjacent crystallites, strongly contribute to the strength of a semicrystalline polymer.[13] It follows that a polymer is brittle if its density of intercrystalline links is too low to transmit the stress required to plastically deform the crystallites.[12,40] The density of intercrystalline links is believed to depend both on intrinsic properties of the polymer (i.e., mainly the chain length for a linear polymer) and on crystallization conditions.[41] Typically, annealing near the melting point embrittles semicrystalline polymers, in particular owing to a decrease in the number of intercrystalline links. Indeed, during slow crystallization, the chains can disentangle during their folding in crystal lamellae, which diminishes the density of intercrystalline links.[42]

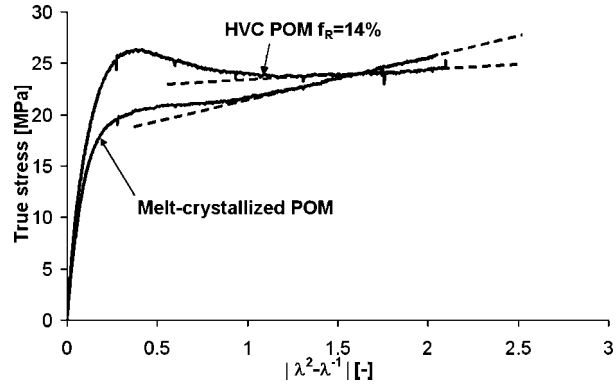

Figure 11. True stress versus $\lambda^2 - \lambda^{-1}$ from POM compressive test at 130 °C.

Regarding nascent crystallization, it has been suggested that polymerization conditions influence the density of intercrystalline links. The key parameters seem to be the density of active catalyst sites, the polymerization rate and the crystallization rate. If the density of catalyst sites is low, the growing polymer chains are separated from each other and the formation of entanglements is difficult, especially if crystallization is fast and simultaneous with polymerization.[3,6]

It has been shown that nascent UHMWPE generally exhibits entanglements,[7,8] except in very particular polymerization conditions,[8,43] which is not surprising considering its very high molecular weight. No information is available concerning nascent POM, but its very high crystallinity leads to suspect a low density of intercrystalline links.

The density of intercrystalline links has been related to several mechanical properties such as creep[44] or strain hardening.[45,46] For amorphous polymers, it is well accepted that the strain hardening is related to the network density (entanglements or cross-links).[47] Schrauwen et al.[45] and Bartczak et al.[46] have successfully extended this idea to semicrystalline polymer strain hardening. It has been shown that the strain hardening modulus does not depend on crystallinity degree and is only related to molecular topology, i.e. the density of intercrystalline links. Following this approach, compressive tests were carried out on HVC and melt-crystallized POM samples, at 130 °C to ease crystal plasticity. The stress has been plotted versus $\lambda^2 - \lambda^{-1}$ (λ is the extension ratio) in Figure 11. Indeed, Gaussian model of chain extension predicts that stress is linear in $\lambda^2 - \lambda^{-1}$ during strain hardening,[14,48] which has been experimentally observed on amorphous and semicrystalline polymers.[45,47] HVC POM and melt-crystallized POM exhibit a completely different behavior after the yield. HVC POM (principally composed of nascent material) shows a marked strain-softening followed by a plateau, and no (or delayed) strain hardening, while melt-crystallized POM shows no strain softening but a significant strain hardening from 40% true strain. The difference in strain hardening behavior reveals that HVC POM likely has a very low density of intercrystalline links. This lack of crystalline links probably originates in the simultaneous crystallization and polymerization. In addition it will tend to increase after HVC, owing to disentanglement during the thickening process and also because the probability of forming tie molecules decreases with increasing l_c.[13,49]

NB: the same compressive tests have been conducted for UHMWPE and contrarily to POM hardening has been observed for a HVC material at $f_R = 13\%$. It confirms that UHMWPE nascent powder intrinsically contains a sufficient density of tie molecules to allow the development of crystal plasticity.

4.2. Conclusion: A Two-Scale Structure. It appears that HVC materials are characterized by a very complex structure,

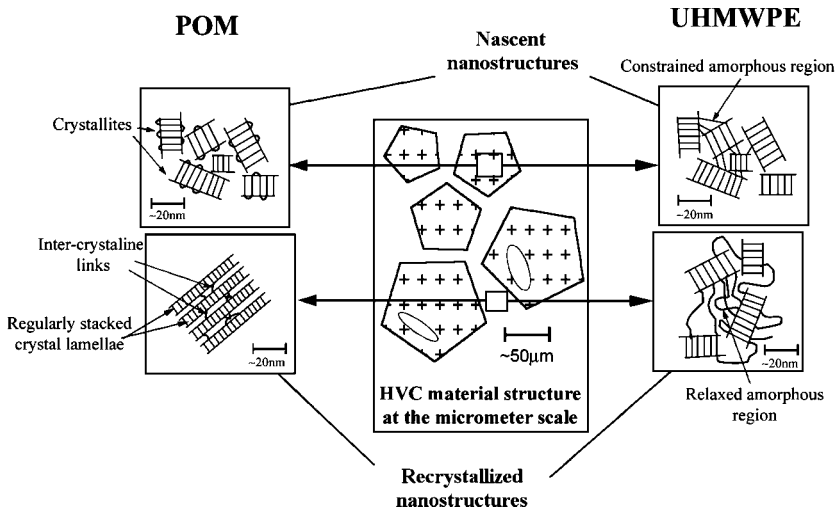

Figure 12. Schematic representation of the two scale structure of HVC processed POM and UHMWPE.

involving two different scales. They are formed, at the micrometer scale, of two different phases; the nascent one and the recrystallized one that are characterized by completely different semicrystalline structures at the nanometer scale.

The common characteristic of the two nascent starting nanostructures is a poorly ordered arrangement of rather small crystallites. Nascent POM seems to have a lack of intercrystalline links, while nascent UHMWPE has a high density of intercrystalline links owing in particular to its very high molecular weight. The evolution of the nascent nanostructures during HVC is characterized by an increase in the average crystal thickness that would contribute to reduce all the more the density of intercrystalline links of HVC POM nascent phase.

Ultimately, the complete melting of the nascent polymer will be reached locally and will lead to the formation of the recrystallized phase upon cooling. It is thought that the nascent particularly high crystallinity would only be lost after this local melting. In the case of POM, the recrystallization would occur in the form of regular stacks of lamella; hence the low degree of order is also lost. For UHMWPE the topological constrains causing the specific nascent melting behavior would be erased, but the very long chains would hinder the recrystallization in regular stacks of lamellae. A schematic representation of the different structures deduced from our investigation is provided in Figure 12.

5. Consequences on Mechanical Properties

In light of the complex microstructure of HVC materials, now well characterized, it is attempted to explain the mechanical behavior of these materials. Extensive studies concerning mechanical characterization of HVC material can be found in our previous studies.[10,11] True stress−true strain curves from compression tests are provided in Figure 13 to summarize the differences in stiffness, yield stress and failure behavior between HVC materials and melt-crystallized materials. HVC materials are both stiffer and have a higher yield stress than their melt-crystallized counterpart. However, they exhibit a different failure behavior at ambient temperature. HVC POM is intrinsically brittle and even in compressive stress state it fails at very low strains, while HVC UHMWPE exhibits a significant ductility.

5.1. Young's Modulus. POM and UHMWPE processed by HVC exhibit a very high Young's modulus that varies with the fraction of recrystallized material.[11] A plot of Young's modulus versus recrystallized phase fraction f_R shows that the evolution is linear, which has a physical sense and correspond to a parallel mechanical coupling of the nascent phase and the recrystallized

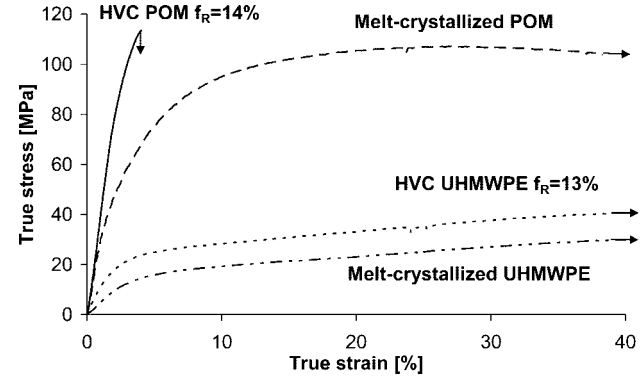

Figure 13. Compressive fracture behavior of HVC and melt-crystallized material at 20 °C. For HVC materials, f_R are similar, in order to have an equivalent overall sintering.

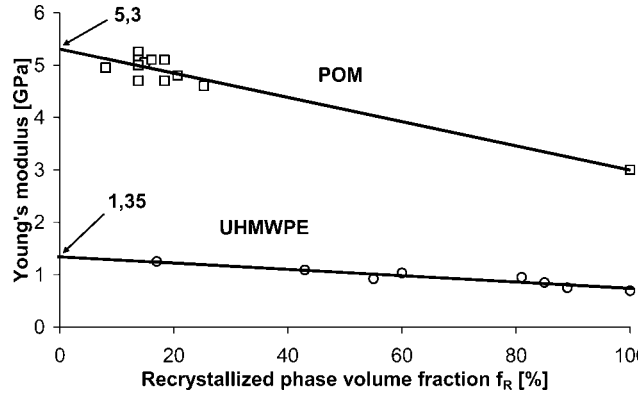

Figure 14. Young's modulus versus recrystallized phase fraction. Points at $f_R = 100\%$ correspond to melt-crystallized material. Straight lines are fitted to data.

phase (Figure 14). As there is only a little difference between the moduli of the two phases, a series model or other model (Takayanagi model[14] for example) would also fit the data. By an extrapolation, it is possible to obtain the Young's modulus of the nascent materials that for both POM and UHMWPE reveals to be nearly twice higher than that of melt-crystallized materials. It is consistent with nanoindentation measurements which have also revealed that nascent phases are nearly twice stiffer.[9,33] The stiffness of the nascent phase is governed by its local crystal weight fraction. A slight crystallinity increase can greatly improve the modulus of a semicrystalline polymer by a

direct effect of the crystallinity degree but also by an indirect effect of the morphology (e.g., increased crystal contiguity at high crystallinity degrees).[4,50,51] The higher elastic modulus of nascent phase is thus undoubtedly due to higher crystallinity, but probably also the particular nanostructure of the nascent material in which crystallite percolation could be more important.

5.2. Yield Stress and Plastic Deformation. POM and UHMWPE containing nascent phase show systematically a higher yield stress than conventionally processed materials. Observations by scanning electron microscopy of fracture surfaces have shown that the recrystallized phase reaches its yield before the nascent phase: fibrils resulting in extensive plastic deformation of recrystallized phase are observed while nascent phase shows limited deformations. Therefore it is thought that nascent phase has a very high yield stress and reinforces HVC materials, explaining their higher yield stress.[9] The origin of this higher yield stress will now be discussed in light of the established knowledge concerning the complex yield stress−nanostructure relationships.

Semicrystalline yield stress has often been related to crystal thickness. On a theoretical point of view, considering thermal nucleation of screw dislocation within the crystalline lamella, Young has predicted that yield stress of a crystal lamella depends on its thickness.[52] Young's model generally accounts for the experimentally observed yield stress increase with crystal thickness.[53−55] Crystallographic slip is not the only mechanism involved in semicrystalline polymer yielding. The deformation of amorphous component (i.e., interlamellar slip, lamellar separation and stack rotation) also contributes to the overall deformation during the yield.[55,56] There is a combined deformation of both amorphous and crystal components, and therefore the crystallinity degree should also influence the yield stress independently of crystal thickness. It has to be noted that.

Here, in addition to the higher crystallinity of nascent POM, the lamellae of HVC POM nascent phase are thicker than melt-crystallized ones, which easily explain the higher yield stress of this phase. However, in the case of UHMWPE, nascent crystallites seem to stay thinner than melt-crystallized ones, even after HVC (Figures 3 and 4), and therefore the higher yield stress can hardly be explained in term of increased crystal thickness. The effect of the crystallinity is believed to be limited[46] but could nevertheless partially account for the yield stress increase. In addition, the correlation between crystal thickness and yield stress has been established for regularly stacked lamellae and do not necessarily apply for the very specific and complex nascent UHMWPE structure. Indeed, poorly ordered nascent crystals can form, together with constrained amorphous phase, stiff aggregates that could need higher stress to activate crystallographic plasticity than predicted by Young theory for regularly lamella stacks. Nascent UHMWPE could also contain a small fraction of extended chain crystals,[57] that would likely be preserved after HVC. This small amount of thick crystals would probably not increase significantly the average crystal thickness obtained by SAXS but could lead to an increase in the yield stress.

5.3. Fracture Behavior. True stress−true strain curves from compression tests displayed in Figure 13 show that HVC UHMWPE is ductile while HVC POM is brittle, reaching only 4% strain in our experimental conditions. In the same conditions injected POM exhibit an elongation at fracture about 10 times higher. The compressive stress state limits the influence of possible local poorly welded interfaces (i.e., sintering defects) that could provoke a premature failure. In addition, the behavior difference between POM and UHMWPE is observed for similar f_R. It is thus believed that this behavior difference is intrinsic to nascent phases. This has been confirmed by a simple test

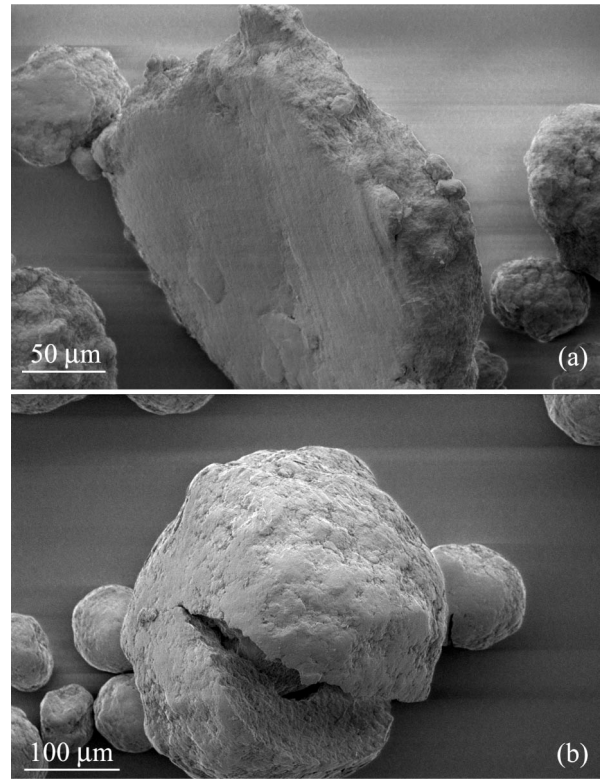

Figure 15. LVSEM observation of nascent particles crushed at ambient temperature. (a) Nascent UHMWPE GUR 4113. (b) Nascent POM Delrin 500.

that consists in crushing nascent polymer powder particles and observing the resulting deformation under LVSEM. This test reveals that nascent UHMWPE particles are highly ductile, while nascent POM ones are brittle, i.e., exhibit cracking before large deformation (Figure 15). It has to be noted that many particles have been crushed and all of them have been found to be fragile. The crack is systematically in the middle of the particle which corresponds to the maximum of tensile stress. Moreover, fractured surfaces on HVC POM containing high fraction of nascent phase has been observed by ESEM. Large flat surfaces have been observed which indicates that the crack goes through many particles without being deviated by possible defects.[10] Therefore we can be confident in drawing conclusions concerning the intrinsic behavior of the material.

Semicrystalline polymers break in a brittle manner when intercrystalline links cannot transmit the stress necessary to generate plasticity.[12,39] It follows that nascent POM brittleness is likely due to a combined effect of its high yield stress and its low density of intercrystalline links. Concerning nascent UHMWPE, although having a high yield stress, it exhibits significant ductility owing to a high density of intercrystalline links. It has to be noted that mechanical response of semicrystalline polymers strongly depends on $T/T_{\alpha c}$ where T is the test temperature and $T_{\alpha c}$ is the crystal relaxation temperature. They are different for POM and UHMWPE (the $T_{\alpha c}$ peaks are respectively about 50 and 130 °C at 1 Hz). Then additive crush tests have been carried out at 100 °C for POM and the brittle behavior was again observed whereas POM is known to be ductile a this temperature. It confirms the intrinsic brittleness of nascent POM.

6. Conclusion

Thanks to a new process (high velocity compaction) it has been possible to take advantage of crystalline structure of nascent powders directly extracted from the polymerization

reactor. From nascent powders of POM and UHMWPE, bulk materials containing and adjustable rate of nascent phase and recrystallized phase have been obtained. The microstucture of these so-called "auto-composite" materials exhibits at a micrometric scale nascent zones and recrystallized zones. It has been shown that the crystallinity of the nascent phase is significantly higher than the recrystallized one. In addition SAXS analysis has shown that these structures are less organized leading possibly to a better percolation of the crystallites. High crystallinity and possible better percolation explain the very high Young's modulus of the nascent phase. At a lower scale, it seems that crystalline growth during polymerization is facilitated which explains the high crystallinity. However, it leads also to a lower rate of tie molecules. For POM (relatively short chains) this effect induces brittle behavior of the nascent phase whereas for UHMWPE (very long chain) it is counterbalanced by the chain length and the nascent phase remains ductile.

As HVC material are autocomposites, the recrystallized phase is reinforced by the nascent phase, explaining its higher Young's modulus and Yield stress. However the global ductility is decreased in particular for POM where nascent structure is brittle.

From this study, it clearly appears that the nature of the nascent material has a strong influence on final properties of HVC material. Nascent material for HVC processing should exhibit both high crystallinity and high density of intercrystalline links to obtain final material with highly valuable mechanical properties. Studies on nascent UHMWPE have shown that density of intercrystalline links can be controlled by polymerization conditions. However, the relationships between polymerization conditions and nascent nanostructure are not fully understood and some work should be performed in this field to be able to synthesize optimized nascent polymer powders dedicated to the HVC process.

References and Notes

(1) Wang, X. Y.; Salovey, R. *J. Appl. Polym. Sci.* **1987**, *34*, 593–599.
(2) Hofmann, D.; Schulz, E.; Fanter, D.; Fuhrmann, H.; Bilda, D. *J. Appl. Polym. Sci.* **1991**, 42.
(3) Loos, J.; Arndt-Rosenau, M.; Weingarten, U.; Kaminsky, W.; Lemstra, P. J. *Polym. Bull.* **2002**, *48*, 191–198.
(4) Al Jebawi, K.; Sixou, B.; Seguela, R.; Vigier, G.; Chervin, C. *J. Appl. Polym. Sci.* **2006**, *102*, 1274–1284.
(5) Joo, Y. L.; Han, O. H.; Lee, H. K.; Song, J. K. *Polymer* **2000**, *41*, 1355–1368.
(6) Joo, Y. L.; Zhou, H.; Lee, S. G.; Lee, H. K.; Song, J. K. *J. Appl. Polym. Sci.* **2005**, *98*, 718–730.
(7) Ivan'kova, E. M.; Myasnikova, L. P.; Marikhin, V. A.; Baulin, A. A.; Volchek, B. Z. *J. Macromol. Sci., Part B: Phys.* **2001**, *40*, 813–832.
(8) Rastogi, S.; Lippits, D. R.; Peters, G. W. M.; Graf, R.; Yao, Y.; Spiess, H. W. *Nat. Mater.* **2005**, *4*, 635–641.
(9) Jauffrès, D.; Lame, O.; Vigier, G.; Doré, F. Presented at *EPF2007*, Portoroz, Slovenia, 2007.
(10) Jauffrès, D.; Lame, O.; Vigier, G.; Doré, F.; Chervin, C. *J. Appl. Polym. Sci.* **2007**, *106*, 488–497.
(11) Jauffrès, D.; Lame, O.; Vigier, G.; Doré, F. *Polymer* **2007**, *48*, 6374–6383.
(12) Brown, N.; Ward, I. M. *J. Mater. Sci.* **1983**, *18*, 1405–1420.
(13) Seguela, R. *J. Polym. Sci., Part B: Polym. Phys.* **2005**, *43*, 1729–1748.
(14) Ward, I. M.; Sweeney, J. *Mechanical properties of solid polymers*; 2nd ed.; Wiley: London, 2004.
(15) Tervoort-Engelen, Y. M. T.; Lemstra, P. J. *Polym. Commun.* **1991**, *32*, 343–345.
(16) Uehara, H.; Yamanobe, T.; Komoto, T. *Macromolecules* **2000**, *33*, 4861–4870.
(17) Egorov, V. M.; Ivan'kova, E. M.; Marikhin, V. A.; Myasnikova, L. P.; Drews, A. *J. Macromol. Sci.: Part B: Phys.* **2002**, *B41*, 939–956.
(18) Lippits, D. R.; Rastogi, S.; Hohne, G. W. *Phys. Rev. Lett.* **2006**, 96.
(19) Rastogi, S.; Lippits, D. R.; Hohne, G. W.; Mezari, B.; Magusin, P. C. M. M. *J. Phys.: Condens. Matter* **2007**, *19*, 205122.
(20) Al Jebawi, K.; Sixou, B.; Seguela, R.; Vigier, G. *J. Appl. Polym. Sci.* **2007**, *106*, 757–764.
(21) Sixou, B.; Al Jebawi, K.; Seguela, R.; Vigier, G. *e-Polym.* **2007**.
(22) Lindner, P.; Zemb, T. *Neutron, X-ray and light scattering*; North-Holland: Amsterdam, 1991.
(23) Wunderlich, B. *Macromolecular physics*; Academic Press: New York, 1980.
(24) Brandrup, J.; Immergut, E. H.; Bloch, D. R.; Gruckle, E. A. *Polymer Handbook*; 4th ed.; Wiley: New York, 1999.
(25) Goderis, B.; Reynaers, H.; Koch, M. H. J.; Mathot, V. B. F. *J. Polym. Sci.: Part B: Polym. Phys.* **1999**, *37*, 1715–1738.
(26) Slusarczyk, C. *J. Alloys Compds.* **2004**, *382*, 68–74.
(27) Magonov, S. N.; Godovsky, Y. *Am. Lab.* **1999**, *April*, 52–58.
(28) Ottani, S.; Ferracini, E.; Ferrero, A.; Malta, V.; Porter, R. S. *Macromolecules* **1995**, *28*, 2411–2423.
(29) Bellare, A.; Schnablegger, H.; Cohen, R. E. *Macromolecules* **1995**, *23*, 7585–7588.
(30) Marega, C.; Marigo, A.; Causin, V. *J. Appl. Polym. Sci.* **2003**, *90*, 2400–2407.
(31) Song, H. H.; Wu, D. Q.; Chu, B.; Satkowski, M.; Ree, M.; Stein, R. S.; Phillips, J. C. *Macromolecules* **1990**, *23*, 2380–2384.
(32) Hsiao, B. S.; Sauer, B. B.; Verma, R. K. *Macromolecules* **1995**, *28*, 6931–6936.
(33) Jauffres, D.; Lame, O.; Vigier, G.; Doré, F.; Douillard, T. Manuscript in preparation **2007**.
(34) Petermann, J.; Miles, M.; Gleiter, H. *J. Macromol. Sci.: Part B: Phys.* **1976**, *12*, 393–404.
(35) Strobl, G. *Eur. Phys. J. E* **2000**, *3*, 165–183.
(36) Heck, B.; Hugel, T.; Iijima, M.; Strobl, G. *Polymer* **2000**, *41*, 8839–8848.
(37) Bartczak, Z.; Lezak, E. *Polymer* **2005**, *46*, 6050–6063.
(38) Sauer, B. B.; McLean, R. S.; Londono, J. D. *J. Macromol. Sci.: Part B: Phys.* **2000**, *38*, 519–543.
(39) Mihailov, M.; Nedkov, E.; Terlemezyan, L. *Polymer* **1980**, *21*, 66–70.
(40) Zhang, X. C.; Butler, M. F.; Cameron, R. E. *Polymer* **2000**, *41*, 3797–3807.
(41) Keith, H. D.; Padden, F. J. J.; Vadimsky, R. G. *J. Polym. Sci.: Part B: Polym. Phys.* **1966**, *4*, 267–281.
(42) Plummer, C.; Béguelin, P.; Kausch, H. H. *Polym. Eng. Sci.* **1995**, *35*, 1300–1312.
(43) Smith, P.; Chanzy, H. D.; Rotzinger, B. P. *J. Mater. Sci.* **1987**, *22*, 523–531.
(44) Cazenave, J.; Seguela, R.; Sixou, B.; Germain, Y. *Polymer* **2006**, *47*, 3904–3914.
(45) Schrauwen, B. A. G.; Jansen, R. P. M.; Govaert, L. E.; Meijer, H. E. H. *Macromolecules* **2004**, *37*, 6069–6078.
(46) Bartczak, Z.; Kozanecki, M. *Polymer* **2005**, *46*, 8210–8221.
(47) Van Melick, H. G. H.; Govaert, L. E.; Meijer, H. E. H. *Polymer* **2003**, *44*, 2493–2502.
(48) James, H. M.; Guth, E. *J. Chem. Phys.* **1943**, *11*, 455–481.
(49) Janimak, J. J.; Stevens, G. C. *J. Mater. Sci.* **2001**, *36*, 1879–1884.
(50) St Lawrence, S.; Shinozaki, D. M. *J. Mater. Sci.* **1998**, *33*, 4059–4068.
(51) Crist, B.; Fisher, C. J.; Howard, P. R. *Macromolecules* **1989**, *22*, 1709–1718.
(52) Young, R. J. *Philos. Mag.* **1974**, *30*, 85–94.
(53) Seguela, R. *e-Polym.* **2007**, no. 32.
(54) Brooks, N. W. J.; Mukhtar, M. *Polymer* **2000**, *41*, 1475–1480.
(55) Oleinik, E. F. *Polym. Sci. Ser. C* **2003**, *45*, 17–117.
(56) Hiss, R.; Hobeika, S.; Lynn, C.; Strobl, G. *Macromolecules* **1999**, *32*, 4390–4403.
(57) Cook, J. T. E.; Klein, P. G.; Ward, I. M.; Brain, A. A. F. F. D.; Rose, J. *Polymer* **2000**, *41*, 8615–8623.

MA801133V